Astron. Astrophys. 140, 303–313 (1984)

ASTRONOMY AND ASTROPHYSICS

^{13}CO in the inner galactic plane

H.S. Liszt[1], W.B. Burton[2], and D.-L. Xiang[1,3]

[1] National Radio Astronomy Observatory, Edgemont Road, Charlottesville, VA 22901, USA
[2] Sterrewacht Leiden, Postbus 9513, NL-2300 RA Leiden, The Netherlands
[3] Purple Mountain Observatory, Nanking, China

Received September 15, 1983; accepted May 2, 1984

Summary. We have mapped ^{13}CO emission at λ 2.7 mm along the galactic plane from $l = 20\overset{\circ}{.}5$ to $40\overset{\circ}{.}0$, extending the earlier survey of Liszt et al. (1981b). These observations are used to discuss three topics. 1) The ratio of emissivities $A\,^{12}\mathrm{CO}/A\,^{13}\mathrm{CO}$ varies by more than a factor 2 across the galactic disk. The variations mimic those seen for extinction across local clouds, indicating a lower mean hydrogen column density for clouds observed at larger galactocentric radii. 2) Analysis of terminal velocities measured on ^{13}CO and H I profiles is used to constrain the cloud mean free path and cloud-cloud random velocity dispersion σ_{cc}. We show that $\langle\sigma_{cc}\rangle = 4.2$ km s^{-1} and that there is no net flow of the molecular ensemble with respect to the atomic gas. A statistical analysis of some 200 local cloud velocities observed at $|b| \geqq 1\overset{\circ}{.}5$ yields $\langle\sigma_{cc}\rangle = 4.5$ km s^{-1}. 3) We model the effect of cold H I in molecular clouds on low-latitude inner-galaxy 21-cm H I profiles. Even rather thick molecular-cloud H I has only small effects upon H I intensity integrals (5%), derived mean densities (15%), and terminal velocities (0.5 km s^{-1}); the model profiles are, however, heavily distorted near the terminal velocity, exposing several types of analyses to subsequent dangers.

Key words: galactic structure – molecular clouds – interstellar absorption – interstellar clouds – H I

I. Introduction

The past decade has seen several extensive surveys of carbon monoxide emission from the galactic molecular cloud ensemble. For practical reasons, the largest of these currently available, by Burton and Gordon 1978; Sanders et al., 1984; Cohen and Thaddeus, 1983; and Robinson et al. 1983, deal exclusively with the most abundant ^{12}CO isotope; relatively few survey observations of ^{13}CO have appeared (see Scoville and Solomon, 1980 and Liszt et al. 1981b, our Paper I), and these have been of limited coverage and extent. Nonetheless it is recognized that some combination of observations of two or more isotopic species is crucial to the determination of cloud column densities. Although weaker than ^{12}CO emission, even by itself ^{13}CO emission offers several advantages stemming from its narrower, less heavily saturated lines which facilitate separation of individual cloud contributions. In Paper I we exploited this situation to derive the size and mass distribution of molecular clouds, from which we estimated the total molecular mass in the inner regions of the galactic disk.

Here, we present an extension of the earlier ^{13}CO survey, comprising spectra at $b = 0'$ at 3′ spacing over the longitude range $20\overset{\circ}{.}5 \leqq l \leqq 40\overset{\circ}{.}0$. We use these observations, partly in conjunction with the work of Burton and Gordon (1978), to discuss several properties of molecular clouds. In Sect. III we show that there is a continuous variation across the galactic disk in the ratio of abundances $A\,^{12}\mathrm{CO}/A\,^{13}\mathrm{CO}$. We argue that this behaviour, which results in changes in the emissivity ratio of a factor two, arises from a larger mean column density per cloud nearer the peak of the molecular annulus than elsewhere. Similar behaviour is observed with varying extinction across individual local clouds. In Sect. IV we consider the statistics of CO and H I terminal velocities in the inner galaxy and conclude that the molecular cloud kinematics may be understood better if the kinematic effects of observing a clumpy medium are taken into account. The two isotopic species have identical large-scale behaviour in the sense that there is no net relative motion of the two constituents. We derive values for the characteristic molecular cloud mean free path ($\lambda = 1.7$ kpc) and cloud-cloud velocity dispersion ($\sigma_{cc} = 4.2$ km s^{-1}) which are in accord with our earlier work (Liszt and Burton, 1981). We show that a sample of some 200 lines of sight toward local material observed away from the galactic equator yields a value of 4.5 km s^{-1} for the dispersion in the Solar vicinity. In Sect. V we model the effects of cold H I in molecular clouds upon the low-latitude λ 21 cm H I profiles observed by Burton et al. (1978) and Liszt et al. (1981). The molecular clouds strongly affect H I profile shapes, but induce only rather mild changes in integrated line intensity or terminal velocity.

II. Observations and definitions

The ^{13}CO observations include those of Liszt et al. (1981b), and a newly observed extension between $l = 20\overset{\circ}{.}5$ and $27\overset{\circ}{.}8$ taken in March 1981. The Kitt Peak 11-m antenna was thus used at $0\overset{\circ}{.}05$ spacings to accumulate 391 spectra in the region $b = 0°$, $20\overset{\circ}{.}5 \leqq l \leqq 40\overset{\circ}{.}0$. The data are shown in Fig. 1 in the form of a longitude-velocity diagram. A few additional spectra taken out to $l = 46°$ at $0\overset{\circ}{.}2$ spacings are shown in Fig. 3 below, but are not otherwise discussed. Integration times of 6 to 10 minutes resulted in 3σ noise levels of 0.1 K at our spectral resolution of 0.5 MHz or 1.36 km s^{-1}. The CO intensities discussed here are in terms of T_A and have not been scaled upward to account for geometric coupling of the antenna response pattern to the source emission.

Send offprint requests to: W.B. Burton

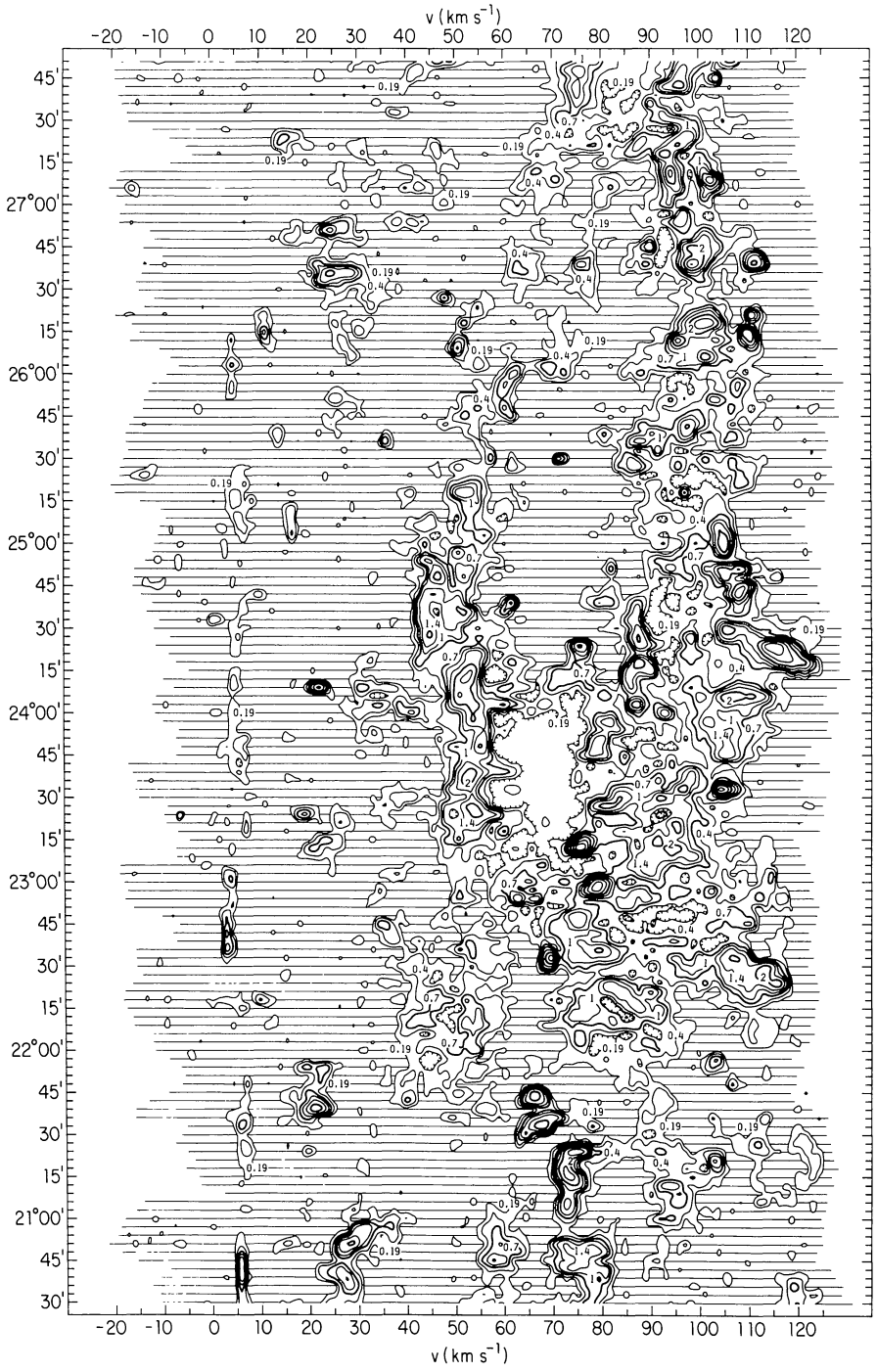

Fig. 1a. Longitude-velocity diagram of ^{13}CO emission in the galactic plane between $l =$ 20°.5 and 27°.8. The contours give T_A at 0.19, 0.4, 0.7, 1.0, 1.4, 2.0, 2.5, 3.0, 4.0, ... K. The diagram is comparable to the ones for $l =$ 27°.8 to 40°.0 given in Paper I

We remind the reader that the 11-m antenna had a broad error-pattern which affected galactic-plane observations in a manner which for many purposes should not be neglected (cf. Liszt and Burton, 1981). For observations of the sort discussed here, the nominal beam efficiency is probably of order 0.8 or more, higher than the value 0.65 corresponding to the main forward lobe alone.

In this paper we employ the integrated emissivity $A\,^{13}CO$ and $A\,^{12}CO$, defined as the summed, integrated emission from an annulus in galactocentric radius R, divided by the total path length sampled by the observations in that annulus. Units of A are thus K km s^{-1} kpc^{-1}. Velocities are converted to galactocentric radius using the rotation curve given by Burton and Gordon (1978), which incorporates the still-current IAU values of $R_0 =$ 10 kpc and $\theta_0 = 250$ km s^{-1}. The velocities are expressed relative to the local standard of rest motion of 20 km s^{-1} toward α, $\delta =$ 18^h, +30° (epoch 1900.0). The integrated emission from a single cloud, $\int T_A\,dv$, is denoted by I_{12} or I_{13}, depending on the isotope intended.

III. Gradients in cloud properties across the galactic disk

The observational characteristics of molecular clouds are no doubt determined by many influences. On the largest scales in

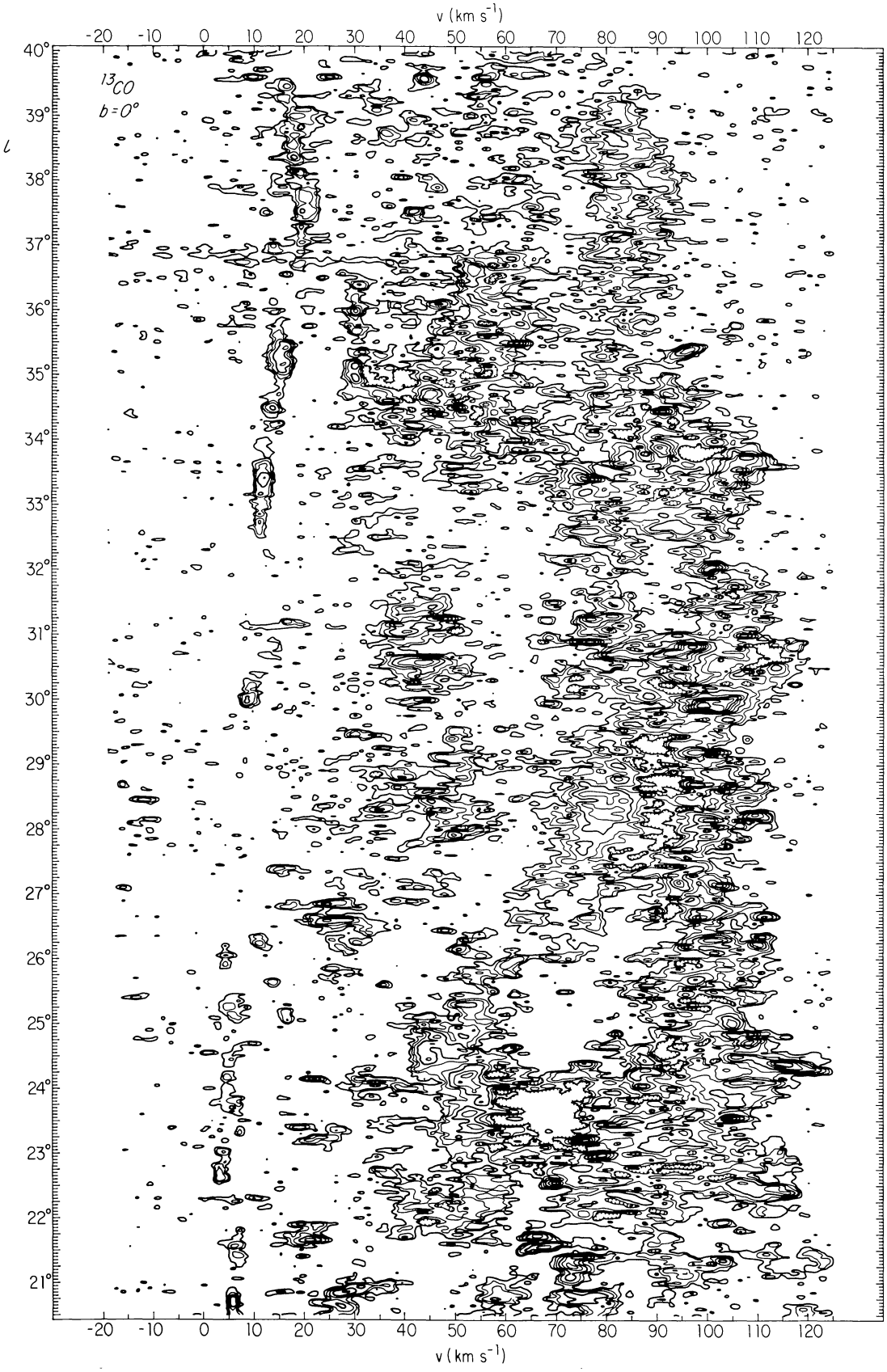

Fig. 1b. Longitude-velocity diagram of ^{13}CO emission in the galactic plane between $l = 20.^{\circ}5$ and $40.^{\circ}0$, combining that data in Fig. 1(a) with that given in Paper I. The contour levels are the same in all cases

the cloud ensemble the time between cloud collisions, eventual passage through galactic-scale shocks, and the overall matter density, among other influences, will be important. On the scale of individual clouds, the local environment, including such matters as the ambient fluxes of photons and particles, will be important, as will be the cloud density, temperature and chemical composition, and the stage of star formation within the cloud. Differences in mean cloud properties across the galactic disk are therefore to be expected on a variety of grounds, but have not been identified in previous molecular survey work.

One aspect of variation in CO emission properties is shown in Fig. 2a, in which we give histograms of molecular emissivity A ^{12}CO and A^{13}CO and their quotient as a function of galactocentric radius. The main-isotope observations are taken from the coarser survey of Burton and Gordon (1978) over the longitude range sample in ^{13}CO, but scaled by a factor 0.7 in intensity in order to bring them into agreement with other published results and with a set of 15 calibration spectra taken in March 1981. The ratio of ^{12}CO–to–^{13}CO emissivities varies substantially with galactic radius, rising on both sides of the peak of the molecular annulus and increasing by more than a factor two across the galactic disk. It is important to decide which physical property is responsible for this variation.

The systematic behaviour of the ratio of emissivities does not reflect a change in the carbon isotope ratio bound up in carbon monoxide, as studies of this ratio in various molecules have failed to find any such effect (Wannier, 1980; Penzias, 1980). We note also that cloud blending, which more seriously affects the thicker, broader ^{12}CO line, should act in the direction of the observed changes. Our observations mainly sample the peak of the molecular distribution near the very crowded terminal velocity, where blending is severe, even in ^{13}CO spectra. To check this possibility, we ran simulations of the ensemble in both isotopes following the methods of Liszt and Burton (1981), but found only very weak effects (5–10%) in the ratio. This result is consistent with earlier claims by us and others that cloud blending or shadowing influences perceived cloud sizes much more strongly than it does the integrated intensities. It is much more likely that the wings of spectral features will overlap, because of their larger extent in velocity, than that there will be overlap of the higher-opacity central spectral peaks.

The decline in molecular emissivity at both larger and smaller galactocentric radii suggests that the ^{12}CO/^{13}CO emissivity ratio may be plotted as a function single-valued in *emissivity*; this is shown in Fig. 2b. There are at least two ways to understand the observed behaviour. Blitz and Shu (1980) suggested that increases in metallicity and CO abundance in the inner galactic regions would generally raise the CO intensity for a given cloud mass, resulting in smaller inferred cloud masses of H_2. It is further to be expected that larger CO column densities would be more directly reflected in the weaker, thinner isotopes, resulting in the lower emissivity ratio observed. However, the line intensities of ^{12}CO and ^{13}CO scale rather weakly with abundance, being typically observed in the ratio 5–10:1 (compared with their 60:1 column density ratio). Models of molecular clouds predict intensity variations for ^{13}CO which in the present context vary roughly as the square-root of the ^{13}CO/H_2 ratio (Liszt et al. 1981b), necessitating very large increases in this quantity in order to account for the observations. These increases are much larger than those proposed by Blitz and Shu (1980).

Differing cloud *structures* will have an important influence on CO emission properties. The observations can be interpreted rather straightforwardly in such terms. We note that the variations seen in the emissivity ratio mimic those seen for integrated line intensities in local clouds. Larger ratios I_{12}/I_{13} are observed at smaller values of the visual extinction or at smaller values of I_{13}. In Fig. 2c we show the ratio I_{12}/I_{13} plotted against A_V and I_{13} for two local clouds recently studied in many CO isotopes by Frerking et al. (1982). The systematic behaviour of the local cloud emission is quite similar to that seen across the galactic disk. We therefore find it plausible that it is the mean cloud column density which changes over the galactic disk and which dominates the observed variation of the emissivity ratio with R.

We have attempted to reinforce this conclusion by plotting the survey data for a constant value of the cloud mean free path

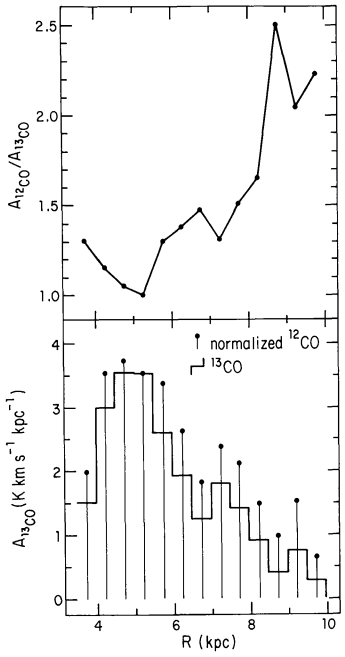

Fig. 2a. Radial variation of the ^{12}CO and ^{13}CO emissivities (bottom panel) and their quotient (top). The ^{12}CO data and the quotient have been normalized at $R = 5.25$ kpc.

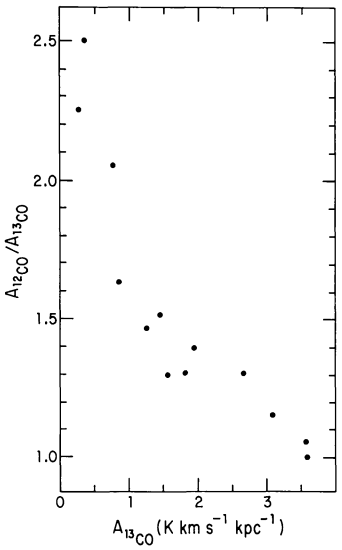

Fig. 2b. Ratio of emissivities from Fig. 2a plotted against the ^{13}CO emissivity rather than against R

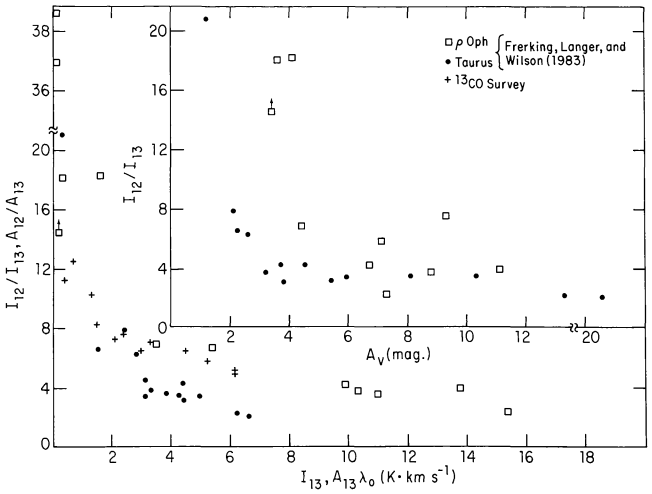

Fig. 2c. Ratio of integrated line strengths in ^{12}CO and ^{13}CO for the Taurus and Ophiucus clouds as functions of visual extinction (inset) and ^{13}CO line strength I_{13} (Frerking et al., 1982). The galactic survey data are plotted using a single value of the cloud mean free path $\lambda_0 = 1.7$ kpc as discussed in Sect. III of the text, and behave as in the local cloud material.

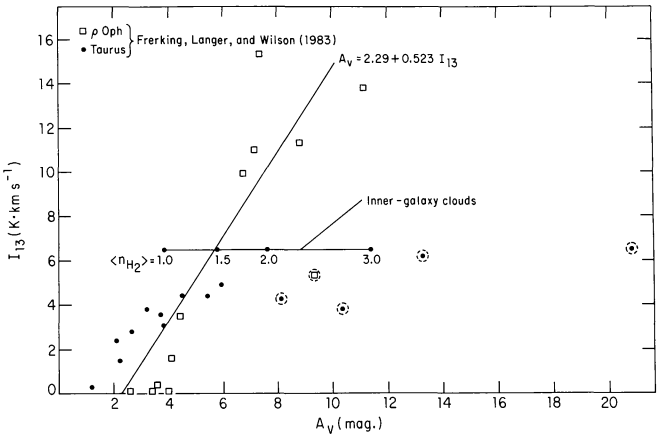

Fig. 2d. Variation of integrated line strength I_{13} with extinction for the Taurus and Ophiuchus clouds. The horizontal line shows the mean extinction per cloud required to yield the indicated space-averaged molecular hydrogen densities (Sect. III of the text). The regression line $A_v = 2.29 + 0.523\ I_{13}$ was constructed using the non-circled data points

$\lambda_0 = 1.7$ kpc. Because the cloud mean free path increases with galactocentric radius, crosses at the left in this Figure are plotted somewhat too far to the left, but it is a consequence of this discussion that the cloud mean free path at larger galactocentric radii is rather less than previously supposed. If the mean integrated emission from the survey clouds is taken to be constant with galactocentric radius, it follows that $\lambda \alpha A_{CO}^{-1}$. Modelling of the galactic cloud ensemble has usually used this proportionality (although without serious consequences because most of the inferences concerned inner-galaxy material); in this case the survey data shown in Fig. 2c would appear, implausibly, along a single vertical line. In the region covered by our survey, both the ^{12}CO and ^{13}CO contributions per cloud are less at lower velocity, and the cloud mean free path locally is not actually four or more times longer than in the inner galaxy. This important matter should be quantified using the more extensive latitude coverage of other surveys now in progress (see Sanders et al., 1984).

The suggestion that the changes in integrated emissivity across the Galaxy reflect changes in matter density in the clouds implies that other observed properties of the clouds may also vary. Increased density implies for example more efficient star formation and consequently hotter clouds. This interpretation is consistent with the earlier suggestions of Cesarsky et al. (1977) that a possible gradient across the Galaxy of the extent to which cosmic rays penetrate molecular clouds is relevant to interpretation of the observed gamma-ray morphology. Cesarsky et al. also discuss the consequences in this regard of a possible variation across the Galaxy of the abundance of ^{13}CO relative to H.

This interpretation is also consistent with the results of Kutner and Meade (1981), reporting colder, more weakly emitting clouds at large R; there is considerable uncertainty regarding the observations of Kutner and Meade (see Solomon et al., 1983), although the general conclusion may be valid.

One further aspect of the survey measurements can also be placed straightforwardly in the context of local cloud observations, i.e., the mean density of molecular material in the inner galaxy. In Fig. 2d we have plotted the variation of integrated line strength I_{13} with extinction across the Taurus and Ophiuchus clouds as determined by Frerking et al. (1982). Placed in this plane is the locus of mean extinction per cloud required to yield a given space-averaged mean density of H_2 at the z- and R-peak of the molecular annulus. We take $I_{13} = A\ ^{13}\mathrm{CO}\ \lambda_0 =$ 3.6 1.7 K km s^{-1}, a value measured from our work in the galactic equator which should be z-invariant (see Sect. IV for a discussion of the mean free path, or that in Liszt and Burton, 1981). Because the z-distribution of the inner-galaxy molecular material peaks somewhat away from the $b = 0.^{\circ}0$ longitude sampled here (see Sanders et al., 1984), we take as approximate compensation a somewhat shorter value of the mean-free-path parameter, $\lambda =$ 1.3 kpc. We convert extinction to H_2-column density using $N_H =$ 2 10^{21} cm^{-2} mag^{-1}. The mean density is proportional to $\langle A_V \rangle / \lambda$. The mean extinction is varied in the plot.

Our purpose here is to demonstrate that the use of differing parameters for local clouds has not, by itself, distorted the derived values of the mean molecular density in the inner galactic regions as suggested by Blitz and Shu (1980; see their Fig. 1a). The densities $\langle n_{H_2} \rangle \simeq 2.0$ H_2 cm^{-3} which have been inferred to exist there (Liszt et al., 1981b; Burton and Gordon, 1978) are consistent with the intensities of molecular clouds seen locally; all of the substantial possible errors indicated by the positions of observations in the Figure would *increase* the mean density. Based on this comparison, we believe that the downward revision in density posited by Blitz and Shu (1980) is largely inapplicable to most recently quoted mean molecular densities; we do note, however, that the densities ~ 5 H_2 cm^{-3} originally derived by Solomon and collaborators (Scoville and Solomon, 1975; Solomon and Sanders, 1980) are now recognized by them to have been substantial overestimates (cf. Sanders et al., 1984). Aspects of the determination of the molecular mass of the Galaxy from observations of ^{12}CO and ^{13}CO have recently been reviewed by Liszt (1984).

IV. The cloud-to-cloud random velocity

The parameters of the molecular cloud ensemble which most directly determine its appearance in our survey are the cloud

mean free path $\lambda(R)$ and the one-dimensional line-of-sight velocity dispersion σ_{cc}. The latter is taken to represent only the locally defined random motions found in a comparatively small volume element, and as such contains no contributions representing systematic deviations from purely rotational motion or other large-scale phenomena. Here, we first discuss a single, easily determined measure which is sensitive to both λ and σ_{cc}: the degree of scatter in the terminal-velocity locus of molecular emission. Analysis of its statistics shows that $\langle\sigma_{cc}\rangle = 4.2$ km s^{-1} in the inner galaxy, with the brackets denoting an average weighted by cloud surface area. Although this value of the dispersion refers to ^{13}CO data, we note that a similar value was found by Burton and Gordon (1978) applying a similar method to earlier ^{12}CO data. Stark et al. (1983) stress the more general conclusion that ^{12}CO and ^{13}CO yield similar cloud statistics. Finally in this section we examine the kinematics of some 200 local cloud observations taken from surveys of CO, and show that the same velocity dispersion pertains to material near the location of the Sun.

A. *Analysis of ^{13}CO terminal velocities*

Material located nearest the sub-central galactocentric distance $R = R_0 \sin(l)$ contributes emission nearest the positive-velocity emission cutoff in the first quadrant. If material is always very common at the sub-central point the observed terminal velocity is determined only by the bulk kinematics of the sub-central region. Such is the case for the atomic hydrogen, which has cloud mean free paths much less than 1 kpc and is adequately characterized for many purposes as a smoothly distributed gas of unit volume filling factor. For cloud mean free paths of 1 kpc or more, the discreteness of the emitting ensemble becomes important. Purely random and typical spatial irregularities may preclude the presence of clouds within several kpc of the sub-central point along a line of sight (sampled over a sufficiently small solid angle), introducing an additional degree of random scatter in the terminal velocity. Thus the scatter is sensitive to both the spatial and kinematic properties of the clouds, allowing derivation of *both* the mean free path and random velocity dispersion from purely kinematic data.

Figure 3 shows the longitude dependence of the terminal velocities measured, following the discussions of Liszt et al. (1981b) and Burton and Gordon (1978), from the ^{13}CO data and from the H I survey of Westerhout and Wendlandt (1982). There is one clear difference between the atomic and molecular gases: the ^{13}CO shows a surfeit of directions having $\delta v = v_{ter}(^{13}\mathrm{CO}) - v_{ter}(\mathrm{H}\ I) \leqq 10$ km s^{-1}. It is these lines of sight which most directly afford a measure of cloud mean free path, and they *cannot* be construed as evidence that the atomic and molecular gases show any significant systematic differences in their kinematics. The terminal velocities of the CO and H I are identical within the limits expected from the clumpiness of the molecular ensemble (having a properly defined mean difference of zero as discussed immediately below). We see no evidence in this measure for gross migration of the molecular clouds with respect to H I. Such a migration has been predicted and discussed in a series of papers by Bash and his collaborators (see for example Bash, 1979).

Figure 4a shows a histogram of the difference δv for the 391 closely space lines of sight at $l \leq 40°$; at higher longitudes, the mean latitude of the sub-central gas drops abruptly away from the galactic equator (Sanders et al., 1983). The distribution is

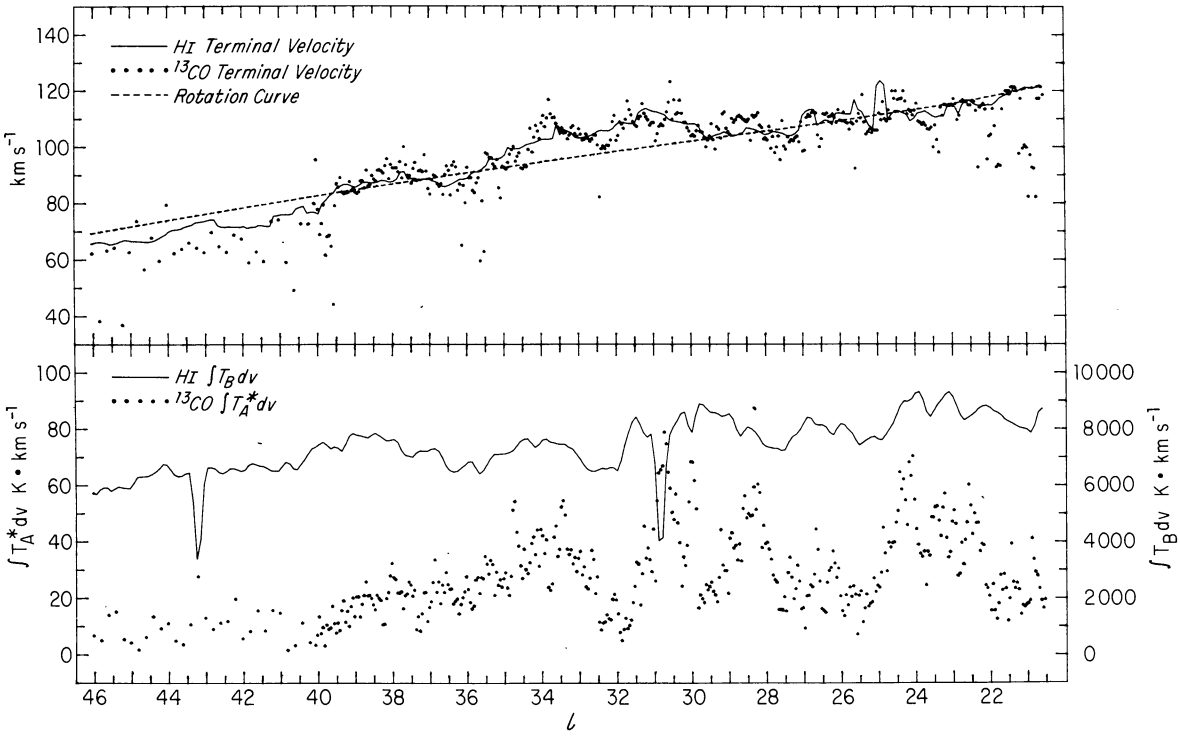

Fig. 3. Longitude variation of H I and ^{13}CO terminal velocities (top panel) and positive-velocity line profile integrals. Except for the presence of absorption dips in the λ21-cm line near H II regions (where the molecular gas is exceptionally strong), there is no statistically significant correspondence between the two sets of line integrals. By contrast, the terminal velocities are highly correlated within the limits imposed by the clumpiness of the molecular cloud ensemble (see Sect. IV of the text)

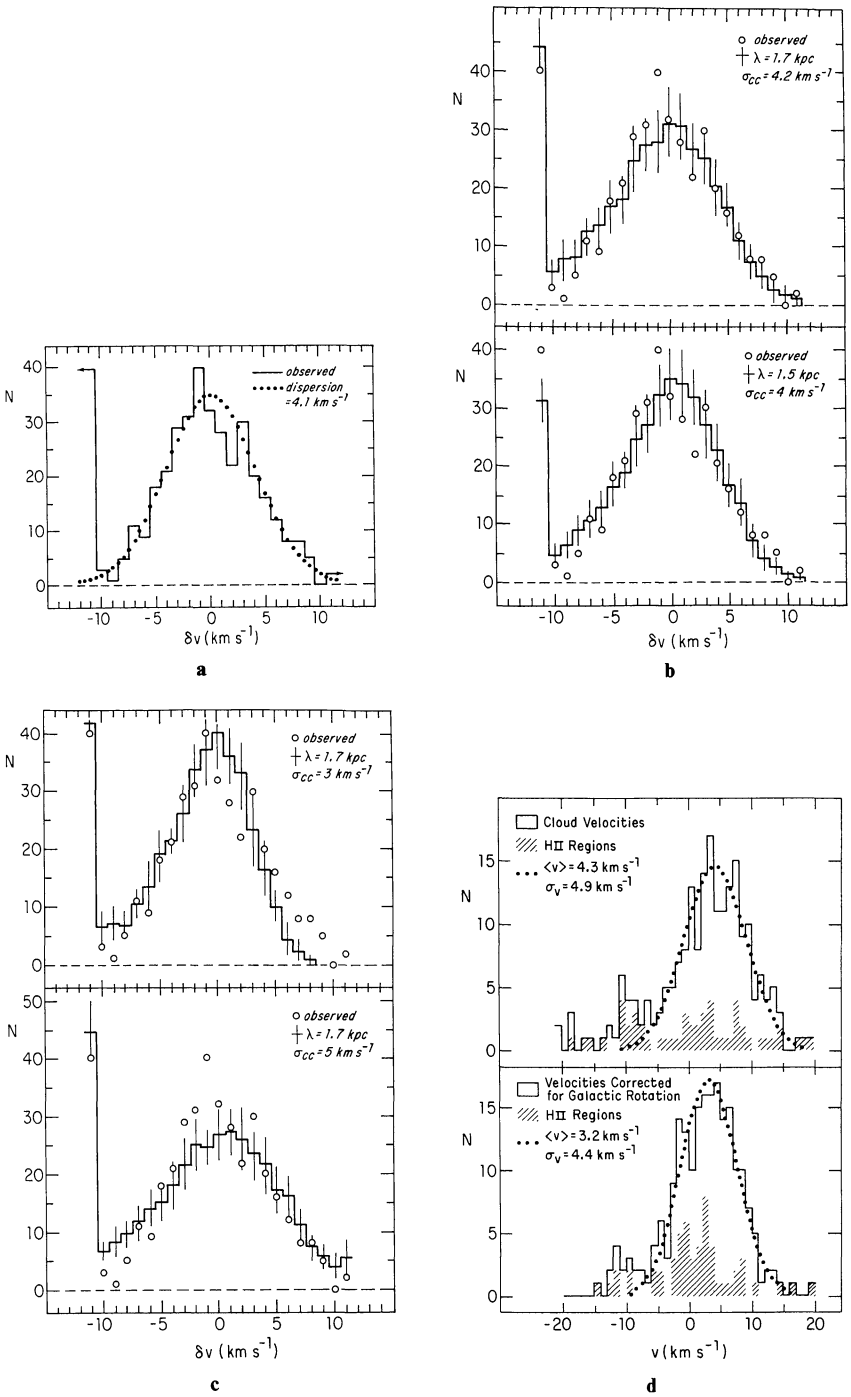

Fig. 4a–d. Kinematical analysis of terminal velocities measured on the H I and ^{13}CO profiles. **a** Histogram of observed differences v_{ter} (^{13}CO) − v_{ter} (H I) at $l \leqq 40°$. The many lines of sight with large, negative differences serve principally to constrain the cloud mean free path; the absence of large positive differences constraints the cloud-cloud velocity dispersion as indicated by the normal distribution, which is shown dotted. Note that there is no relative flow of the atomic and molecular gases. **b** and **c** Results of two-parameter simulations of the observed terminal-velocity statistics for several values of the cloud mean free path λ and cloud-cloud velocity dispersion σ_{cc}. Dispersons as low as 3 km s^{-1} or as large as 5 km s^{-1} provide significantly worse fits to the observation (see Sect. IV of the text). **d** Cloud velocities found along 193 lines of sight toward local molecular material at $|b| \geqq 1.5°$. The expected contribution of galactic rotation has been subtracted in the lower panel. The lines of sight toward H II region complexes from Blitz et al. (1982) are shown hatched

skew at large negative values as would be expected for occasional empty sub-central points; all these data are lumped together in one bin. That there are no such excursions to positive values $\geqq 10$ km s^{-1} shows immediately that $2\sigma_{cc} \leqq 10$ km s^{-1}. The dots in Fig. 4a show a Gaussian function of mean zero (the mean of δv taken over the range $|\delta v| \leq 10.5$ km s^{-1} is 0.3 km s^{-1}) and dispersion 4.1 km s^{-1}. This value of the dispersion has previously been suggested by Burton and Gordon (1978) and Liszt and Burton (1981) to be the actual cloud-cloud line-of-sight velocity dispersion of the inner-galaxy molecular clouds.

To show more quantitatively that this suggestion is correct, and to extract information on the mean free path, we have undertaken a numerical simulation of the observed statistics. The differences δv yield the scatter about the *actual* maximum velocity along the line of sight, given the ubiquity of H I. In our numerical experiment we consider a model Milky Way which is purely rotating (there is no obviously correct model for the actual velocity fields which might usefully be employed in the simulations) and consider the differences $v_{\rm ter}$ (^{13}CO) $- v_{\rm max}$ arising from the clumpiness of the cloud ensemble. That is, we characterize the model molecular galaxy by its rotation curve, mean free path, and velocity dispersion, with the latter two parameters taken as constant over the inner-galaxy regions sampled along the subcentral point. The velocity $v_{\rm max}$ is the radial velocity predicted by the model rotation curve at the subcentral locus. Using one-dimensional Poisson spatial statistics and a random number generator, we find the maximum cloud velocity along the line of sight and form some 1000 ensembles of 391 lines of sight to find the mean histogram and the standard deviation in each of its bins. In order that a function should not be fitted for the mean free path (which varies somewhat with longitude in the data), only the line of sight toward $l = 30°$ was employed. Thus the model involves only two important parameters, the mean free path and the velocity dispersion. The observations could indeed be well fit with this crude, and somewhat tedious, simulation. Fully three-dimensional models require too much computing to be used in the present context, but we have used such three-dimensional simulations in Sect. V to investigate the influence of cold residual H I in molecular clouds on H I emission spectra.

Histograms arising from the simulation are shown in Fig. 4b and 4c. Both the mean and the standard deviation are displayed. The mean free path value of 1.7 kpc is fixed by the number of lines of sight at large negative δv, nearly independently of $\sigma_{\rm cc}$ because the latter is relatively small. The data, which are explicitly binned at lower $|\delta v|$, fix $\sigma_{\rm cc}$ at very nearly the same value as was found from the observational data directly. Values of 3 and 5 km s^{-1} provide substantially worse fits.

There is likely to be some distribution of velocity dispersion among the clouds. If the molecular ensemble were to relax gravitationally, a condition of constant cloud random energy might eventually occur, with the most massive clouds approaching their final $\sigma_{\rm cc}$ most rapidly. For a mass distribution function $f(m) \alpha m^{-\alpha}$ (α is approximately 1.8 in the work of Liszt et al. 1981b and 1.4–1.8 in the theoretical cloud agglomeration models of Kwan 1979 and Cowie, 1980) the condition $m\sigma_{\rm cc}^2 =$ constant implies a dispersion distribution function $f(\sigma_{\rm cc}) \alpha \sigma_{\rm cc}^{2\alpha-3}$. We repeated the numerical simulation using such a distribution and specifying the three additional parameters necessary [α and max, min($\sigma_{\rm cc}$)]. The fit to the data could not be improved substantially; in addition, we confirmed that only a narrow range of cloud random velocity dispersions is permissible because the mean must stay at about 4 km s^{-1}. If the most massive clouds have velocity dispersion of about 3 km s^{-1} (Stark, 1979), the least massive must have $\sigma_{\rm cc}$ not much above 6 km s^{-1}. From our or other available observations it is not possible to discern the funcational relationship of cloud size (or mass) and random velocity and this determination will be difficult. The effects of cloud blending, which act to cause a lower perceived z-scale height for apparently larger clouds observed near the terminal velocity, would also act to produce fewer apparently large clouds at large positive δv as blending must become progressively rarer there. It is important that these effects be addressed, but to do so explicitly requires data densely sampled in latitude as well as in longitude. The most relevant work in this regard is that of Stark (1983, 1984), who does find some indication of dispersion decreasing with increasing apparent cloud size.

We note without further comment two additional points. The values of $\sigma_{\rm cc}$ are rather close to that observed to pertain to H I clouds, 6.2 km s^{-1} (Crovisier, 1978), which the molecular clouds typically out-mass by a factor 10^3. The random velocities of the molecular clouds in the inner galactic regions are just slightly larger than the minimum value required to prevent spontaneous gravitational coalescence.

B. The random motions of local molecular clouds

There is a difference between the typical values of $\sigma_{\rm cc}$ reported here for the inner galaxy and for the Solar vicinity, where a value $\simeq$7 km s^{-1} has been inferred for *massive* clouds on the basis of their mean z-height above the galactic equator (Blitz and Shu, 1980). To explore this matter, we assembled a group of clouds taken from several surveys of more local molecular material, namely those of: Liszt and Burton (1979) and Kazes and Crovisier (1981) who searched for CO toward extragalactic continuum sources with known H I absorption spectra; Kutner et al. (1980) toward reflection nebulae; Blitz et al. (1982) toward H II region complexes; Dickman (1978) toward dark clouds; and an unpublished survey by Liszt who searched for CO toward moderately-reddened stars with well-studied optical and/or UV spectra. We considered only those objects at $|b| \geq 1.5°$ and, for objects with optical distances (the reflection nebulae and many of the H II regions), those within 1.5 kpc. The lines of sight were parsed to eliminate overlap; a group of 193 lines of sight was retained. The observed velocities are shown in Fig. 4c; they can be seen to have a central distribution with $\langle v \rangle \simeq 4$ km s^{-1}, $\sigma_v \simeq 5$ km s^{-1}. The non-zero mean is not just an artifact of longitude distribution as 115 of the 193 lines of sight lie in the second and fourth quadrants. Rather, it signifies the "expansion" of the local cloud system. This is a well-known peculiarity of the local kinematics (see e.g. Lindblad, 1967; Dieter, 1973, and Burton and Bania, 1974).

To derive the cloud-cloud velocity dispersion more precisely it is necessary to account for the expected contribution of galactic rotation (cf. Crovisier, 1978). For clouds with known distances, this process is direct. For the remainder of the clouds we performed a statistical solution in two variables, namely the mean absolute z-height and longitude node. This yielded a very nominal z-dispersion of $\simeq$40 pc (all clouds were assumed to lie at the same distance $\langle |z| \rangle$ from the galactic plane) and nodal deviation of only 10°. The corrected distribution of velocities is shown in the lower panel of Fig. 4d, and its indicated $\sigma_{\rm cc}$ is nearly identical to that obtained in the inner-galaxy analysis. The subtraction of galactic rotation does little to lower the mean velocity or to narrow the central velocity distribution, but most of the highest velocities are greatly reduced in this process.

We conclude, in a dynamical sense, that the observed z-dispersion is somewhat open to question. When spatial distributions are converted to velocity dispersions using the expected vertical deceleration, as by Blitz and Shu (1980) or by Stark (1979), it is sometimes the case that higher values are inferred than can be directly observed, a situation which is not unique to the molecular material. Using the K_z value given by Spitzer (1978), one finds, locally, that $\sigma_z \simeq 9\sqrt{2}$ pc $(\sigma_v / 1$ km s$^{-1})$, the factor $\sqrt{2}$ arising from inclusion of cosmic-ray and magnetic pressures. The velocity dispersion of molecular material is

sufficient to provide for a 40–60 pc z-dispersion locally, which is very close to the values observed slightly interior to the Sun (Solomon and Sanders, 1980; Sanders et al., 1984). At yet smaller radii, where the mean matter density in the plane should be greater, and at larger ones, where the z-distribution of interstellar gas broadens appreciably, this dynamical consistency is less apparent. The local velocity dispersion of H I absorbing material, 6.2 km s^{-1}, would provide a z-dispersion of $\leqq$80 pc, while the value inferred from statistical kinematic analysis is at least 50% larger (Crovisier, 1978). There is some indication that τ_{cc} may be larger in the outer galaxy than the value which we derive locally and for the molecular annulus (see Stark, 1984).

V. Cold H I in molecular clouds

Molecular clouds manifest themselves in H I survey observations such as those used in Fig. 3 because there appears to be an important fraction of residual atomic hydrogen inside the cold, dense material (Burton et al., 1978; Liszt et al., 1981a). At temperatures of 15 K, even one percent of the hydrogen column density corresponding to 5 magnitudes of visual extinction will give an optically thick H I line for linewidths comparable to those observed in dark or molecular clouds.

At least two important influences have been ascribed to such gas. It has been argued that the presence of cold, high-optical depth clouds diminishes the perceived H I column density at low latitudes to such an extent that the comparison of molecular and atomic gas densities in the inner galaxy is seriously compromised (Dickey and Benson, 1982). In addition, the peculiar shape of H I profiles observed at longitudes 25° to 40°, in which the highest brightness temperatures occur well below the terminal velocity, has been explained in terms of blanketing by cold material in molecular clouds; it is precisely in this region that the molecular annulus appears at the subcentral point (Liszt et al., 1981a).

Cold, optically thick atomic gas in molecular clouds will induce scatter in the longitude variation of the H I line integral and terminal velocity; systematically, the line integral will be depressed and the measured terminal velocity raised when the definition of the latter following Shane and Bieger-Smith (1966) is employed. The increase arises because the measurement process is affected only when distortion of the profile occurs at or above the (normal) high-velocity peak and because the line temperatures near the high-velocity peak will always be affected more strongly than the line integral beyond them.

To find out how much havoc the molecular clouds could wreak upon the H I profiles, we ran a three-dimensional cloud simulation in which 25-pc molecular clouds were distributed over the disk, immersed in a diffuse all-pervasive H I gas, and observed with an 8′ Gaussian beam at 0°.4 intervals at longitudes 15° to 60°. The properties of the residual, cold, cloud-confined H I were temperature (15 K), internal velocity dispersion (1.3 km s^{-1}), and central optical depth (1.5, corresponding roughly to 1% of the column density of a typical cloud). The diffuse medium in the simulation had temperature 135 K, velocity dispersion 6 km s^{-1}, and number density 0.38 cm^{-3}, parameters which would, in the absence of the clouds, account for most general properties of the observed brightness temperatures. The clouds were distributed so that the mean free path at the peak of the molecular annulus was 1.3 kpc (but following the probably incorrect radial variation inversely proportional to the ^{12}CO abundance to keep the number of clouds manageable); the average main free path over the regions of the model galactic disk sampled was 3 kpc. The integrated H I opacity per kpc of path due to the clouds was 2.7 km s^{-1} at the peak of the annulus; locally, and apparently at fairly large distance (Dickey et al., 1981), the integrated opacity of all H I clouds is 5.5 km s^{-1} kpc^{-1}.

We found that the H I confined to molecular clouds affects previously stated results only slightly. The mean H I intensity integral is lowered by 5% (from a mean of 6500 K km s^{-1}) and a point-to-point scatter of 110 K (an rms value averaged over all longitudes) is introduced. The mean density of H I derived from the synthetic profiles after correction for optical depth effects at 135 K is reduced by 5–15%, depending on radius as shown in Fig. 5a. The mean H I terminal velocity is increased by just 0.3 km s^{-1} (0.5 km s^{-1} over the longitude range sampled here in CO) and a point-to-point scatter of 0.5 km s^{-1} is introduced (0.7 km s^{-1} over the narrower range). None of these effects is serious enough, in the present context, to warrant much consideration.

There is, however, one effect of the residual molecular-cloud H I which *is* liable to influence substantially some galactic structure analyses. The opacity of such material blankets and consequently distorts the high-velocity portions of inner-galaxy H I profiles. Shown in Fig. 5b are two line profiles arising in the simulation. At lower longitudes, where the diffuse gas gives a low-velocity peak, the molecular opacity is effective in shifting the highest intensity to lower velocities than would be expected for the cloud-free gas. At higher longitudes, the terminal-velocity intensity ridge is too strong to be removed by blanketing. Shown in Fig. 5c are optical depth and brightness temperature profiles calculated for a slightly smaller H I dispersion, 4.5 km s^{-1}: the purpose here is to demonstrate how much opacity is required if substantial changes in line intensity are to result from the presence of a cold H I component having a mean free path as long as that of the molecular material. Alternatively, a component having (in the mean) only a few percent of the total H I accounts for about half the opacity found at the higher velocities. The integrated H I optical depth per kpc should not be expected to show the same behaviour with galactocentric radius as either the line brightness or the true number density. The most important practical consequence of the profile distortions caused by the cold H I probably are to be found in galactic morphology studies. For example, Gaussian decomposition, or other decompositions of the profiles based on isolating peaks and valleys for the purpose of tracing large-scale structure, may give suspect results.

While it would not be surprising if the characteristics of H I clouds were different in the inner-galaxy, there are other influences which might also act to produce the observed profile shapes. The terminal velocity ridge is weaker when a realistic distribution of cloud opacities and spin temperatures is used to model the H I (because higher optical depth H I clouds are colder, as discussed by Liszt, 1983 and by Payne et al., 1983, and because the atomic gas has a volume filling factor which is substantially below unity). Kinematics may also play a role; intensity increases at lower velocities can be produced by streaming motions in the galactic disk. It should also be noted that many locally-observed H I self-absorption features due to cold gas lying in dark clouds are apparently not accompanied by detectable CO emission even though the clouds themselves are presumably composed mainly of molecular gas (Levinson and Brown, 1981). In considering only one cloud component we may have underestimated the effects of dark and molecular material.

With regard to comparison of the atomic and molecular gas densities in the inner galaxy, we note that the uniform H I density which reproduces the observed brightness temperatures at 135 K

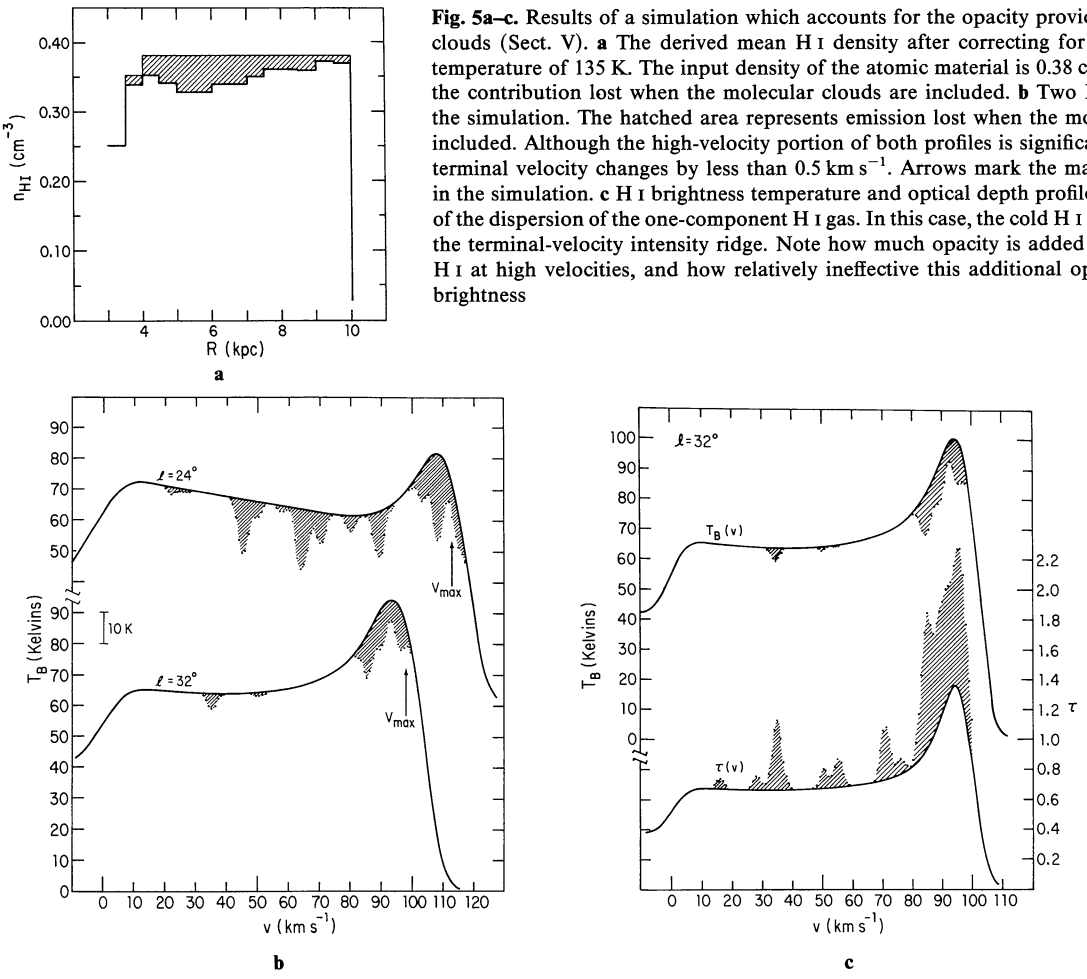

Fig. 5a–c. Results of a simulation which accounts for the opacity provided by cold H I in molecular clouds (Sect. V). **a** The derived mean H I density after correcting for opacity at an assumed spin temperature of 135 K. The input density of the atomic material is 0.38 cm^{-3}; the hatched area shows the contribution lost when the molecular clouds are included. **b** Two H I line profiles arising from the simulation. The hatched area represents emission lost when the molecular cloud line opacity is included. Although the high-velocity portion of both profiles is significantly distorted, the measured terminal velocity changes by less than 0.5 km s^{-1}. Arrows mark the maximum line-of-sight velocity in the simulation. **c** H I brightness temperature and optical depth profiles for a slightly smaller value of the dispersion of the one-component H I gas. In this case, the cold H I is less effective in suppressing the terminal-velocity intensity ridge. Note how much opacity is added by the molecular-cloud cold H I at high velocities, and how relatively ineffective this additional opacity is in reducing the line brightness

has long been known to give an underestimate of the actual atomic gas density in the galactic equator (cf. Baker and Burton, 1975). The mean density of H I is probably about 0.5 cm^{-3} in the plane of the inner galaxy; it is definitely less than 0.7 cm^{-3} (Liszt, 1983) within 1–2 kpc of the Sun. The local surface density of H I is $4.8 \pm 0.8\ M_{\odot}\ \mathrm{pc}^{-2}$ (Liszt, 1983), and it is this quantity to which the inner-galaxy molecular densities may most reliably be compared, there being little change indicated in the H I surface density over most of the inner galactic disk.

Acknowledgements. Research Grant No. 008.82 from the North Atlantic Treaty Organization supports the collaboration of W.B.B. and H.S.L. on inner-galaxy kinematics. The National Radio Astronomy Observatory is operated by Associated Universities, Inc., under contract with the National Science Foundation.

References

Baker, P.L., Burton, W.B.: 1975, *Astrophys. J.* **198**, 281
Bash, F.N.: 1979, *Astrophys. J.* **233**, 524
Blitz, L., Shu, F.: 1980, *Astrophys. J.* **241**, 676
Blitz, L., Fich, M., Stark, A.A.: 1982, *Astrophys. J. Suppl.* **49**, 183
Burton, W. B., Bania, T.M.: 1974, *Astron. Astrophys.* **34**, 75
Burton, W.B., Gordon, M.A.: 1978, *Astron. Astrophys.* **63**, 7
Burton, W.B., Liszt, H.S., Baker, P.L.: 1978, *Astrophys. J. Letters* **219**, L67
Cesarsky, C.J., Cassé, M., Paul, J.A.: 1977, *Astron. Astrophys.* **60**, 139
Cowie, L.B.: 1980, *Astrophys. J.* **236**, 862
Crovisier, J.: 1978, *Astron. Astrophys.* **70**, 43
Dickey, J.M., Rankin, J.M., Weisberg, J.M., Boriakof, V.: 1981, *Astron. Astrophys.* **101**, 332
Dickey, J.M., Benson, J.: 1982, *Astron. J.* **87**, 278
Dickman, R.L.: 1978, *Astrophys. J. Suppl.* **37**, 407
Dieter, N.H.: 1973, *Astrophys. J.* **183**, 449
Frerking, M.A., Langer, W.L., Wilson, R.W.: 1982, *Astrophys. J.* **262**, 590
Kazes, I., Crovisier, J.: 1981, *Astron. Astrophys.* **101**, 401
Kutner, M.L., Machnik, D.E., Tucker, K., Dickman, R.L.: 1980, *Astrophys. J.* **238**, 853
Kutner, M.L., Meade, K.: 1981, *Astrophys. J. Letters* **249**, L15
Levinson, F.H., Brown, R.L.: 1980, *Astrophys. J.* **242**, 116
Kwan, J.: 1979, *Astrophys. J.* **229**, 567
Lindblad, P.O.: 1967, *Bull. Astron. Inst. Neth.* **19**, 34
Liszt, H.S.: 1983, *Astrophys. J.* **275**, 163
Liszt, H.S.: 1984, *Comments on Astrophysics* (*in press*)
Liszt, H.S., Burton, W.B.: 1979, *Astrophys. J.* **228**, 105
Liszt, H.S., Burton, W.B.: 1981, *Astrophys. J.* **143**, 778
Liszt, H.S., Burton, W.B., Bania, T.M.: 1981a, *Astrophys. J.* **246**, 74
Liszt, H.S., Xiang, D., Burton, W.B.: 1981b, *Astrophys. J.* **249**, 532
Payne, H.E., Salpeter, E.E., Terzian, Y.: 1983, *Astrophys. J.* **272**, 540

Penzias, A.A.: 1980, *ISU Symp. No. 87 Interstellar Molecules*, D. Reidel, Dordrecht, p. 397
Sanders, D.B., Solomon, P.M., Scoville, N.Z.: 1984, *Astrophys. J.* **276**, 182
Scoville, N.Z., Solomon, P.M.: 1975, *Astrophys. J. Letters* **199**, L105
Shane, W.W., Biefer-Smith, G.P.: 1966, *Bull. Astron. Inst. Neth.* **18**, 263
Solomon, P.M., Sanders, D.B.: 1980, Giant Molecular Clouds in the Galaxy, Pergamon, New York, p. 41
Solomon, P.M., Scoville, N.Z., Sanders, D.B.: 1983, *Astrophys. J.* **232**, L89
Solomon, P.M., Stark, A.A., Sanders, D.B.: 1983, *Astrophys. J. Letters* **267**, L29
Spitzer, L.: 1978, Physical Processes in the Interstellar Medium, Wiley-Interscience, New York
Stark, A.A.: 1979, Ph.D. Thesis, Princeton Univ
Stark, A.A.: 1984, *Astrophys. J.* (in press)
Stark, A.A.: 1983 in *Kinematics, Dynamics and Structure of the Milky Way*, W.L.H. Shuter, ed., D. Reidel, Dordrecht, p. 127
Stark, A.A., Blitz, L.: 1979, *Astrophys. J. Letters* **225**, L115
Stark, A.A., Penzias, A.A., Beckman, B.: 1983, in *Surveys of the Southern Galaxy*, W.B. Burton, F.P. Israel, eds., D. Reidel, Dordrecht, p. 189
Wannier, P.G.: 1980, *Ann. Rev. Astron. Astrophys.* **18**, 399
Westerhout, G., Wendlandt, H. H.: 1982, *Astron. Astrophys. Suppl.* **49**, 143